

The Ising universality class in dimension three : corrections to scaling

P. H. Lundow

Department of Mathematics and Mathematical Statistics, Umeå University, SE-901 87 Umeå, Sweden

I. A. Campbell

Laboratoire Charles Coulomb (L2C), UMR 5221 CNRS-Université de Montpellier, Montpellier, F-France.

(Dated: March 26, 2019)

Simulation data are analyzed for four 3D spin-1/2 Ising models: the FCC lattice, the BCC lattice, the SC lattice and the Diamond lattice. The observables studied are the susceptibility, the normalized second moment correlation length, and the normalized Binder cumulant. From measurements covering the entire paramagnetic temperature regime the corrections to scaling are estimated. In all four models, for the normalized Binder cumulant the leading confluent correction term has zero amplitude. This implies that the universal ratio of leading confluent correction amplitudes $a_{\chi_4}/a_{\chi} = 2$ in the 3D Ising universality class. An analysis covering all models and observables leads to a numerical estimate of the universal subleading thermal confluent correction exponent $\theta_2 \sim 2.85(10)$ and so the subleading confluent correction exponent $\omega_2 = \theta_2/\nu \sim 4.5$. The value is consistent with the range of values for ω_2 estimated from "bootstrap" theory studies.

I. INTRODUCTION

The development of the "conformal bootstrap" approach has led to a major step forward in understanding the canonical Ising universality class in dimension three [1–6]. The principle universal critical exponents: the correlation length exponent $\nu = 0.62999(5)$, the anomalous dimension $\eta = 0.03631(3)$ (and so the susceptibility exponent $\gamma = (2 - \eta)\nu = 1.23710(12)$ and the specific heat exponent $\alpha = d\nu - 2 = 0.11003(15)$) and the leading confluent correction exponent $\omega = 0.8303(18)$ (and so the thermal confluent correction $\theta = \omega\nu = 0.5231(11)$) are established to high precision. The subleading conformal correction exponents, which are also universal, are not as accurately known. Replacing an earlier estimate, $\omega_2 = 1.67(11)$ so that the thermal exponent $\theta_2 = \omega_2\nu = 1.05(7)$ [7], the bootstrap estimates are $\omega_2 \sim 4.3$ and $\omega_3 \sim 8.6$ so $\theta_2 \sim 2.7$ and $\theta_3 \sim 5.5$ [1–4].

Analyses of simulation data for the 3D universality class (and those of other models) in general focus either on finite size scaling (FSS) at the critical temperature, or on scaling as a function of temperature using the thermal scaling parameter $t = (T - T_c)/T_c$. This approach follows the choice made by K. Wilson who expressed Renormalization Group Theory (RGT) in terms of t . However t obviously diverges at high temperatures, so t scaling can only be used in the near-critical regime. As a result it is widely (and wrongly) believed that critical exponents and intrinsic correction terms can only be estimated from numerical measurements using high precision simulations close to T_c for large sample sizes L . As high order correction terms are only important at temperatures well above criticality, this approach can be ruled out for numerical estimates of subleading conformal correction exponents.

Historically, the standard thermal scaling variable in Ising models was $\tau = (1 - \beta/\beta_c)$ where β is the inverse temperature $1/T$. τ was used initially by Domb and Sykes in 1962 [8], by Wegner for his RGT expan-

sion in 1972 [9], and has been in continuous use in HTSE analyses ever since (see for instance Ref. [10]). τ varies from 0 at criticality to 1 at infinite temperature, with no divergence, so by using τ as the thermal scaling variable HTSE and simulation data can be analysed in detail over the entire paramagnetic temperature regime.

The Wegner expansion for the susceptibility can be written (see for instance Ref. [11] Eqn. 1)

$$\chi(\tau) = C_{\chi}\tau^{-\gamma} (1 + a\tau^{\theta} + b\tau + c\tau^{\theta_2} + \dots) \quad (1)$$

where the leading correction terms only are written explicitly ; the exponents are universal but the critical amplitude C and the correction amplitudes a, b, c are not, though conformal correction amplitude ratios such as a_{χ}/a_{ξ} are universal [12, 13]. The first correction term is the leading confluent correction, the second is the leading analytic correction, and the third one is the subleading confluent correction. Equivalent expressions can be written for other thermodynamic variables $Q(\tau)$ [10]. There is little in the way of *a priori* guidelines as to expected critical amplitudes or correction amplitudes for specific models. A forbidding list of further possible correction terms is indicated for instance by Compostrini *et al.* [14] Eqn. 13, with "minor" terms in $\tau^2, \tau^{\theta+1}, \tau^{2\theta}$ etc. (which can all be considered corrections to corrections). It is noted in Ref. [14] that it can be possible to modify a model Hamiltonian so as to give an "improved" Hamiltonian, where the amplitude of the leading conformal correction term in τ^{θ} becomes zero, for all thermodynamic variables. All the minor correction terms containing factors τ^{θ} will then also be suppressed simultaneously, again for all observables.

The Wegner expansion is for infinite samples, but holds also for finite-size samples in the regime where $L \gg \xi(\tau)$; in practice the rule $L > 7\xi(\tau)$ is sufficient (see for instance Ref. [15]). When this condition holds, $Q(\tau, L)$ data for all L correspond to the infinite- L limit $Q(\tau, \infty)$ and so data for all L coincide. Explicit comparisons between L and $\xi(\tau)$ are generally not needed

to establish where the ThL limit holds, as the ThL regime can be recognized by inspection of data plots for $\chi(\tau, L)$ against τ , or equivalent plots for other observables $Q(\tau, L)$. Once the ThL plots for $Q(\tau, \infty)$ and $\xi(\tau, \infty)$ including the thermal scaling corrections have been established, $Q(\tau, L)$ data for all L and all τ can be concatenated through the Privman-Fisher finite-size scaling rule [16], $Q(\tau, L)/Q(\tau, \infty) = F[L/\xi(\tau, \infty)]$.

It can be noted that at infinite temperature for spin $S = 1/2$ models the susceptibility $\chi(\tau = 1, L) \equiv 1$. It was pointed out [17] that the Wegner expressions for other observables $Q(\tau)$ only take up strictly the susceptibility form if the observable is normalized such that at infinite temperature $Q_n(\tau = 1) = 1$. (Note that with three correction terms this rule imposes the closure condition $C(1 + a + b + c) = 1$). As well as the susceptibility we will study the near-neighbor second-moment correlation length $\xi(\tau)$ and the Binder cumulant $g(\tau)$. $\xi(\tau)$ always tends to $\xi(\tau = 1) = 0$ at infinite temperature, but from the general HTSE series [18] the leading $S = 1/2$ series term for the nearest-neighbor second-moment correlation is $\mu_2(\beta) = z\beta$ where z is the number of near neighbors. So when $\xi(\tau)$ is defined appropriately for the lattice being considered, the normalized correlation length $\xi(\tau)/\beta^{1/2}$ will have an exact high temperature limit $\xi(\tau)/\beta^{1/2} = 1$, and an unaltered critical exponent [17]. This normalized correlation length has a Wegner-temperature dependence

$$\frac{\xi(\tau)}{\beta^{1/2}} = C_\xi \tau^{-\nu} (1 + a_\xi \tau^\theta + b_\xi \tau + c_\xi \tau^{\theta_2} + \dots) \quad (2)$$

with the universal critical exponent ν and with correction amplitudes which, as will be seen below, turn out to be small so the effective ThL normalized correlation-length exponent $\nu(\tau) = \partial \ln[\xi(\tau, L)/\beta^{1/2}]/\partial \ln \tau$ varies little over the entire paramagnetic temperature range.

Assuming hyperscaling, the critical exponent for the second field derivative of the susceptibility $\chi_4(\tau)$ (also called the non-linear susceptibility) is [10]

$$\gamma_4 = \gamma + 2\Delta_{\text{gap}} = D\nu + 2\gamma \quad (3)$$

χ_4 in a cubic lattice is directly related to the Binder cumulant through

$$2g(\tau, L) = \frac{-\chi_4}{L^D \chi^2} = \frac{3\langle m^2 \rangle^2 - \langle m^4 \rangle}{\langle m^2 \rangle^2} \quad (4)$$

see Eq. 10.2 of Ref. [19]. Thus in the ThL regime the normalized Binder cumulant $L^D g(\tau, L) = -\chi_4(\tau, L)/(2\chi(\tau, L)^2)$ scales with a critical exponent $(D\nu + 2\gamma) - 2\gamma = D\nu$. In any $S = 1/2$ Ising system the infinite-temperature (i.e. independent spin) limit for the Binder cumulant is $g(0, N) \equiv 1/N$, where N is the number of spins. As $N = L^D$ for a cubic lattice with L defined appropriately, at infinite temperature $L^D g(\tau, L) \equiv 1$. Thus the 3D normalized Binder cumulant $L^3 g(\tau)$ also obeys the high-temperature limit rule for normalized observables introduced above, and the Wegner expression is

$$L^3 g(\tau, L) = C_g \tau^{-3\nu} (1 + a_g \tau^\theta + b_g \tau + c_g \tau^{\theta_2} + \dots) \quad (5)$$

II. SIMULATIONS AND ANALYSES

We will present data measured over the entire range from criticality to infinite temperature for spin-1/2 Ising models on face centered cubic, body centered cubic, simple cubic, and diamond lattices presented in decreasing order of the number of near neighbors. Most of the data were originally generated for the critical regime analyses of Ref. [20, 21], where the critical temperatures and critical exponents were estimated. The susceptibility up to high temperatures for these lattices (together with others) was presented in Ref. [22] where it was shown that the "crossover" behavior to a high-temperature scaling regime claimed in Refs. [23, 24] was an artefact due to the use by these authors of t as the thermal scaling variable. A detailed analysis of the simple cubic lattice susceptibility and specific heat data along the lines of the present work was described in Ref. [25].

For the four cubic lattices we analyse the data for the susceptibility $\chi(\tau, L)$, the normalized second-moment correlation length $\xi(\tau, L)/\beta^{1/2}$, and the normalized Binder cumulant $L^3 g(\tau, L)$ over the whole paramagnetic temperature regime assuming that in each case the temperature dependence of the observable follows a Wegner expression with a limited set of correction terms, i.e.

$$Q(\tau) = C_q(\tau) \tau^{-\lambda_q} (1 + a_q \tau^\theta + b_q \tau + c_q \tau^{\mu_q}) \quad (6)$$

which is the generalization of Eq. (1), with λ_q standing for the known critical exponent : γ , ν and 3ν respectively, and μ_q is an exponent to be estimated from each of the fits. The amplitudes are also estimated from the fits. All other "minor" correction terms are assumed to have negligible amplitudes. In view of the number of fit parameters we do not attempt to estimate the errors in the individual correction amplitudes. Our final aim is to attempt to determine a unique value for μ consistent with all the data sets. We then identify this μ with the universal subleading exponent θ_2 . (Exceptionally there might be evidence for a further high-order correction term which could be ascribed to corrections with the further exponent θ_3).

To estimate critical amplitudes and the corrections to scaling, simulation data and HTSE data when available can be displayed over the entire paramagnetic temperature regime as $y(\tau) = Q(\tau, L) \tau^{\lambda_q}$ against $x(\tau) = \tau^\theta$. When the leading correction term is the confluent correction with exponent τ^θ this plot is linear at small $x(\tau)$ and the second, analytic, term is nearly proportional to $x(\tau)^2$. This display is appropriate for all the susceptibility and normalized correlation length data. However, we will see that in this universality class, for the normalized Binder cumulant the leading confluent correction term is missing so the appropriate plot becomes $y(\tau)$ against τ . Alternatively for all observables the data can be displayed in the form of an effective temperature-dependent exponent $\lambda_q(\tau) = -\partial \ln Q(\tau, L)/\partial \ln \tau$ [10].

In the latter form of display with the three correction term expression above one has

$$\lambda_q(\tau) = \lambda_q - \frac{a_q \theta \tau^\theta + b_q \tau + c_q \mu \tau^\mu}{1 + (a_q \tau^\theta + b_q \tau + c_q \tau^\mu)} \quad (7)$$

so the limit values are exact : at criticality $\lambda_q(0)$ is by definition equal to the critical exponent : γ , ν or $D\nu$ for the susceptibility, the normalized correlation length, and the normalized Binder cumulant respectively. Close to criticality the leading confluent correction amplitude can be estimated from the initial slope of the $\lambda_q(\tau)$ against τ^θ plot, as [10]

$$\lambda_q(\tau) = -\partial \ln Q(\tau) / \partial \ln \tau = \lambda_q - a_q \theta \tau^\theta \quad (8)$$

In practice this limiting slope is hard to estimate accurately. As a result the values of the universal ratios such as a_χ/a_ξ are only known approximately. For the normalized Binder cumulant $a_g = 0$ (see below) in which case

$$\lambda_g(\tau) = -\partial \ln Q(\tau) / \partial \ln \tau = \lambda_g - b_g \theta \tau \quad (9)$$

With the three correction-term expression above, one has

$$\lambda_q(\tau) = \lambda_q - \frac{a_q \theta \tau^\theta + b_q \tau + c_q \mu \tau^\mu}{1 + a_q \tau^\theta + b_q \tau + c_q \tau^\mu} \quad (10)$$

so at infinite temperature the limiting value becomes

$$\lambda_q(\tau = 1) = \lambda_q - \frac{a_q \theta + b_q + c_q \mu}{1 + a_q + b_q + c_q} \quad (11)$$

At infinite temperature from the leading HTSE series terms [18] one also knows that the $\lambda_q(\tau = 1)$ limiting values are equal to $z\beta_c$, $(z/2)\beta_c$ and $2z\beta_c$ for the susceptibility, the normalized correlation length, and the normalized Binder cumulant respectively where z is the number of near neighbors. These exact limit values are indicated by red arrows in each of the effective exponent plots. These two relations provide an additional closure condition for each observable on the fit correction-term amplitudes together with the fit value for the exponent μ . In particular for the normalized Binder cumulant data with $a_g = 0$ (see below) the parameters C_g and b_g can be read off the critical limit plots; then as $C_g(1+b_g+c_g) = 1$, the infinite temperature limit condition

$$2z\beta_c = 3\nu - (b_g + c_g\mu) / (1 + b_g + c_g) \quad (12)$$

leaves μ fixed.

III. FACE CENTERED CUBIC LATTICE

In this lattice each site has 12 near neighbors and 4 sites per unit cell. The critical inverse temperature

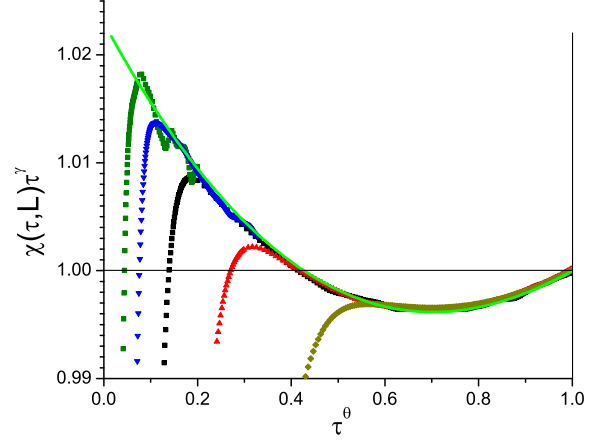


FIG. 1. (Color on line) FCC lattice. Susceptibility data in the form $\chi(\tau, L)\tau^\gamma$ against τ^θ . Data for $L = 128, 64, 32, 16, 8$ from left to right. Green curve is the fit to the ThL data, see Eq. (13).

is $\beta_c = 0.102069(1)$ [21, 26]. The ThL critical amplitudes for the susceptibility and the normalized correlation length $\chi(\tau, L)$ and $\xi(\tau)/\beta^{1/2}$ are both close to 1. The susceptibility data can be fitted satisfactorily with three weak correction terms only : the leading confluent correction $a\tau^\theta$, the leading analytic correction $b\tau$ and the further term $c\tau^\mu$

$$\chi(\tau) = 1.023\tau^{-\gamma} (1 - 0.080\tau^\theta + 0.0595\tau - 0.002\tau^\mu) \quad (13)$$

with $\mu \sim 2.7$, see Figs. 1 and 2.

The normalized correlation length in the ThL regime can also be fitted with three terms only :

$$\frac{\xi(\tau)}{\beta^{1/2}} = 1.0071\tau^{-\nu} (1 - 0.0655\tau^\theta + 0.0635\tau - 0.004\tau^\mu) \quad (14)$$

again with $\mu \sim 2.7$, see Figs. 3 and 4. The effective exponents $\gamma(\tau)$ and $\nu(\tau)$ each vary by only about 1% over the entire temperature range from criticality to infinity. The value $\mu \sim 2.7$ for the tiny third correction term exponents is only rough and will be justified below.

The results for the normalized Binder parameter are more remarkable. The usual leading confluent correction turns out to have zero amplitude and the only visible correction term is the analytic term which is strong and linear in τ . All further higher-order correction terms have negligible amplitudes also, so

$$L^3 g(\tau, L) = 1.614\tau^{-3\nu} (1 - 0.380\tau) \quad (15)$$

As the normalized Binder cumulant is equal to $-\chi_4(\tau)/2\chi(\tau)^2$, the absence of the leading confluent correction term implies that the $\chi_4(\tau)$ and $\chi(\tau)$ confluent correction amplitudes have a ratio $a_{\chi_4}/a_\chi = 2$. Because confluent correction amplitude ratios $a(Q_i)/a(Q_j)$

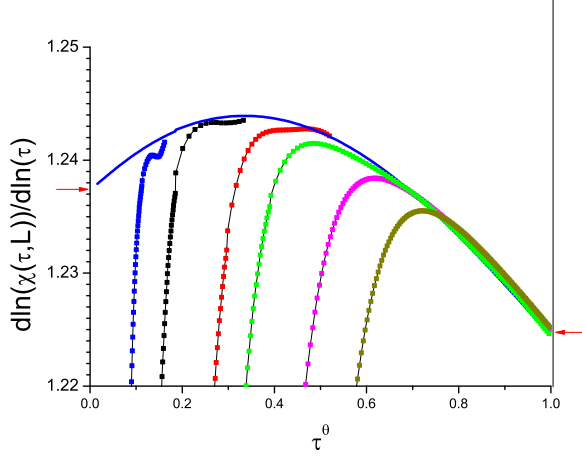


FIG. 2. (Color on line) FCC lattice. The temperature dependent effective susceptibility exponent $\partial \ln \chi(\tau, L) / \partial \ln \tau$ against τ^θ . Data for $L = 64, 32, 16, 12, 8, 6$ from left to right. Green curve is the fit to the ThL data, calculated from $\chi(\tau)$ in Eq. (13).

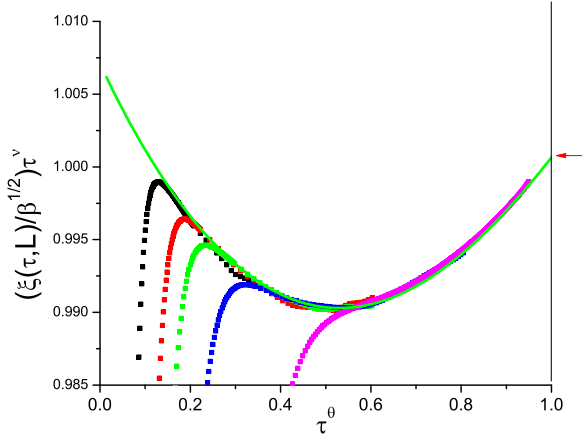


FIG. 3. (Color on line) FCC lattice. Normalized correlation length data in the form $[\xi(\tau, L) / \beta^{1/2}] \tau^\nu$ against τ^θ . Data for $L = 48, 32, 24, 16, 8$ from left to right. Green curve is the fit to the ThL data, see Eq. (14).

are universal [12, 13], the normalized Binder parameter leading confluent correction amplitude will be zero for all models in the 3D Ising universality class. This is indeed confirmed below from the data for the other models studied. For the normalized Binder cumulant all the “minor” correction terms containing factors τ^θ also have zero amplitudes, see Figs. 5 and 6.

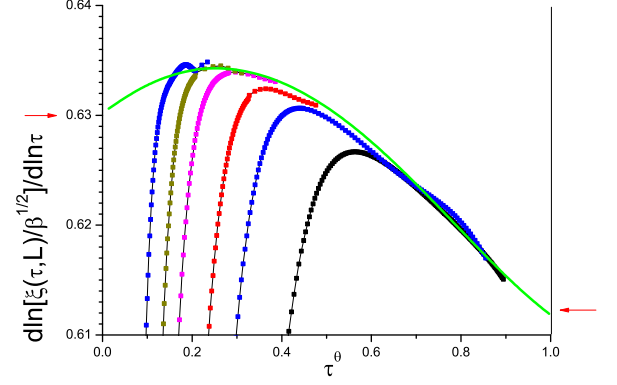


FIG. 4. (Color on line) FCC lattice. The temperature dependent effective correlation length exponent $\partial \ln [\xi(\tau, L) / \beta^{1/2}] / \partial \ln \tau$ against τ^θ . Data for $L = 48, 32, 24, 16, 12, 8$ from left to right. Green curve is the fit to the ThL data, calculated from Eq. (14).

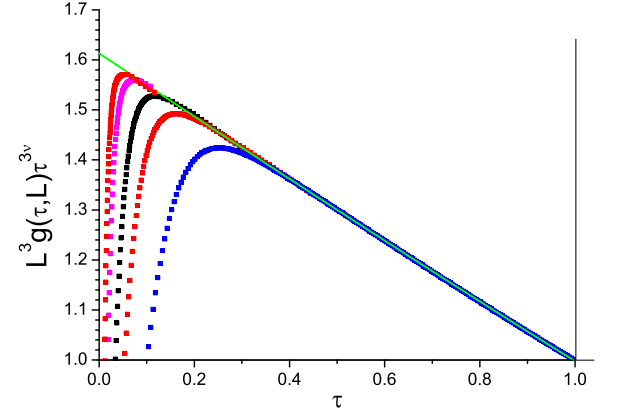


FIG. 5. (Color on line) FCC lattice. Normalized Binder cumulant data in the form $L^3 g(\tau, L) \tau^{3\nu}$ against τ . Data for $L = 32, 24, 16, 12, 8$ from left to right. Green curve is the fit to the ThL data, see Eq. (15).

IV. BODY CENTERED CUBIC LATTICE

In this lattice each site has 8 near neighbors and 2 sites per unit cell. The critical inverse temperature $\beta_c = 0.1573725(5)$ [10, 21, 26]. Extensive lists of exact HTSE terms for this lattice are given in Ref. [18]; we have used these tables to calculate HTSE values for the observables in the high-temperature range where the HTSE sums are essentially exact. Accurate effective exponents to lower temperatures can be obtained by extrapolation [10]. The ThL susceptibility $\chi(\tau, L)$ from simulations and HTSE data can be fitted satisfactorily

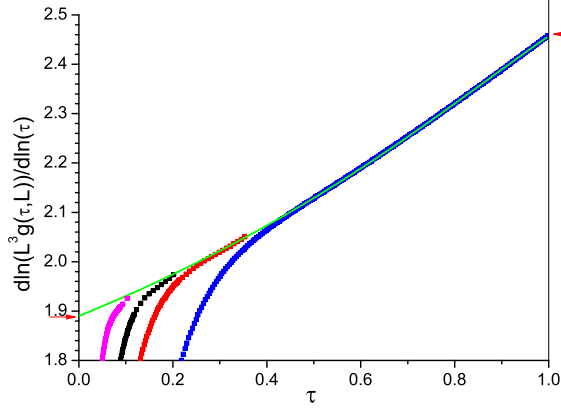


FIG. 6. (Color on line) FCC lattice. The temperature dependent effective normalized Binder cumulant exponent in the form $\partial \ln[L^3 g(\tau, L)]/\partial \ln \tau$ against τ . Data for $L = 24, 16, 12, 8$ from left to right. Green curve is the fit to the ThL data, calculated from Eq. (15).

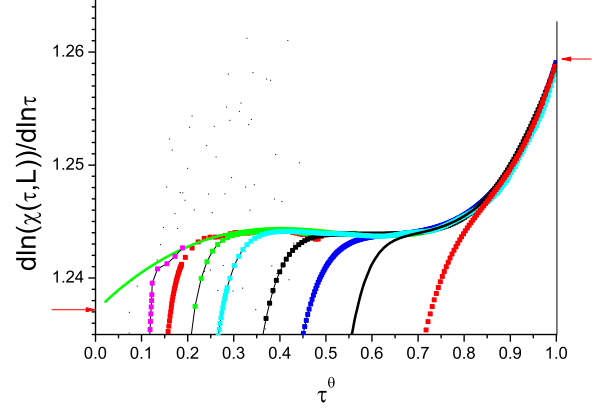


FIG. 8. (Color on line) BCC lattice. The temperature dependent effective susceptibility exponent $\partial \ln \chi(\tau, L)/\partial \ln \tau$ against τ^θ . Data for $L = 64, 48, 32, 24, 16, 12$, HTSE and 6 from left to right. The HTSE curve is a 23 term sum of data from Ref. [18]. Green curve is the fit to the ThL data, calculated from $\chi(\tau)$ in Eq. (16).

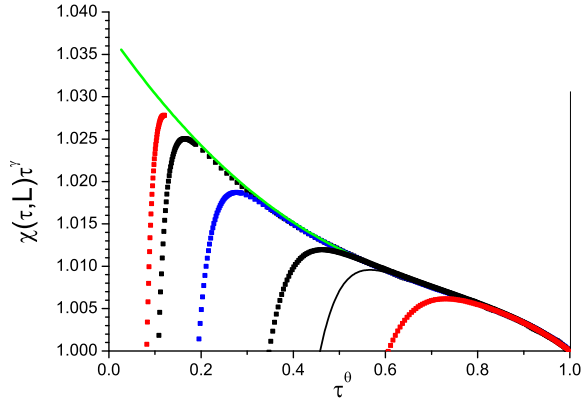


FIG. 7. (Color on line) BCC lattice. Susceptibility data in the form $\chi(\tau, L)\tau^\gamma$ against τ^θ . Data for $L = 96, 64, 48, 24, 12$, HTSE and 6 from left to right. The HTSE curve is a 23 term sum of data from Ref. [18]. Green curve is the fit to the ThL data, see Eq. (16).

with three correction terms :

$$\chi(\tau) = 1.040\tau^{-\gamma} (1 - 0.091\tau^\theta + 0.071\tau - 0.0165\tau^\mu) \quad (16)$$

with $\mu \sim 2.7$, see Figs. 7 and 8.

The fit values for the critical amplitude and the confluent correction amplitude can be compared to those estimated in Ref. [10], $C_\chi = 1.0404(1)$, $a_\chi = -0.129(3)$. The temperature-dependent ThL effective exponent $\gamma(\tau)$ in Fig. 8 is very similar to the $\gamma(\tau)$ curve for the same model shown in Ref. [10] Fig. 16. Because of the opposite signs of the various correction term amplitudes the temperature dependent effective exponent $\gamma(\tau)$ changes

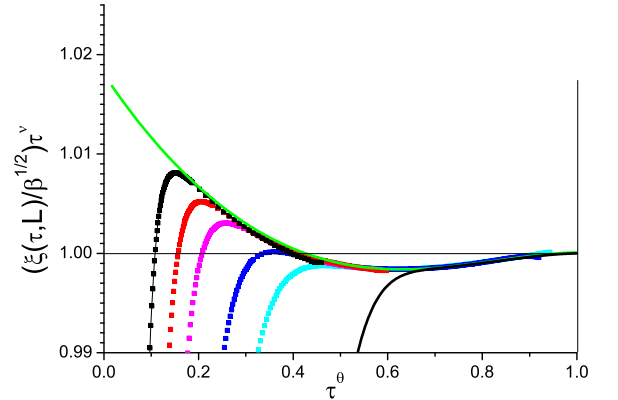


FIG. 9. (Color on line) BCC lattice. Normalized correlation length data in the form $[\xi(\tau, L)/\beta^{1/2}]\tau^\nu$ against τ^θ . Data for $L = 48, 32, 24, 12$ and HTSE from left to right. The HTSE curve is a 23 term sum of data from Ref. [18]. Green curve is the fit to the ThL data, see Eq. (17).

slope twice. The upturns in $\gamma(\tau)$ at high temperatures in both plots correspond to the weak but not negligible negative amplitude correction term with exponent $\mu \sim 2.7$. The normalized correlation length in the ThL regime can also be fitted with three terms :

$$\frac{\xi(\tau)}{\beta^{1/2}} = 1.018\tau^{-\nu} (1 - 0.069\tau^\theta + 0.0619\tau - 0.0102\tau^\mu) \quad (17)$$

with $\mu \sim 2.6$, see Figs. 9 and 10.

The present normalized correlation length critical amplitude C_ξ corresponds to a conventional critical ampli-

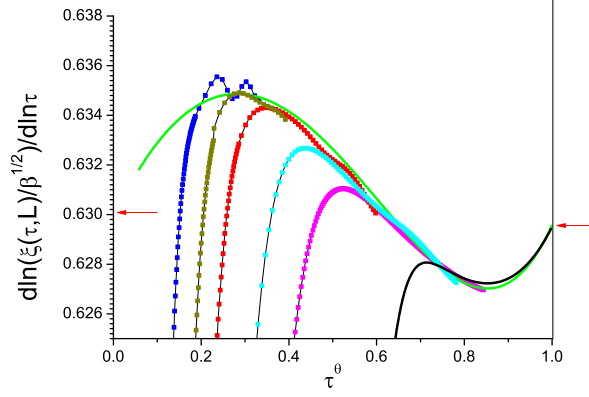


FIG. 10. (Color on line) BCC lattice. The temperature dependent effective correlation length exponent $\partial \ln[\xi(\tau, L)/\beta^{1/2}]/\partial \ln \tau$ against τ^θ . Data for $L = 48, 32, 24, 16, 12$ and HTSE from left to right. The HTSE curve is a 23 term sum of data from Ref. [18]. Green curve is the fit to the ThL data, calculated from Eq. (17).

tude $C_\xi \beta_c^{1/2} = 0.404$. The critical amplitude and confluent correction amplitude can be compared to estimates 0.4681(3) and $-0.100(4)$ in Ref. [10]. The ThL normalized Binder parameter behaves slightly differently from the FCC model. The dominant correction term is again the strong analytic term linear in τ ; however there is a further weak term having an exponent $\mu \sim 2.8$. All other terms are missing including the normal leading correction term in τ^θ and minor correction terms, so :

$$L^3 g(\tau, L) = 1.60\tau^{-3\nu} (1 - 0.365\tau - 0.010\tau^\mu) \quad (18)$$

with $\mu \sim 2.8$, see Figs. 11 and 12.

V. SIMPLE CUBIC LATTICE

In this lattice each site has 6 near neighbors and 1 site per unit cell. The critical inverse temperature is $\beta_c = 0.221654(2)$ [10, 20, 27]. Extensive lists of exact HTSE terms for this lattice are given in Ref. [18]. The ThL susceptibility $\chi(\tau)$ data and the high-temperature HTSE data can be fitted satisfactorily with three correction terms :

$$\chi(\tau) = 1.120\tau^{-\gamma} (1 - 0.112\tau^\theta + 0.0200\tau - 0.016\tau^\mu) \quad (19)$$

with $\mu \sim 2.8$, see Figs. 13 and 14. The fit values for the critical amplitude can be compared to those estimated in Ref. [10], $C_\chi = 1.14(1)$.

The normalized correlation length in the ThL regime can be fitted by

$$\frac{\xi(\tau)}{\beta^{1/2}} = 1.073\tau^{-\nu} (1 - 0.107\tau^\theta + 0.048\tau - 0.0095\tau^\mu) \quad (20)$$

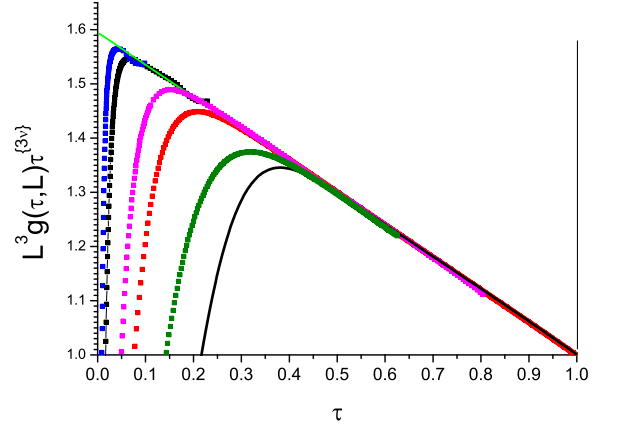


FIG. 11. (Color on line) BCC lattice. Normalized Binder cumulant data in the form $L^3 g(\tau, L)\tau^{3\nu}$ against τ . Data for $L = 48, 32, 16, 12, 8$ and HTSE from left to right. The HTSE curve is a 23 term sum of data from Ref. [18]. Green curve is the fit to the ThL data, see Eq. (15).

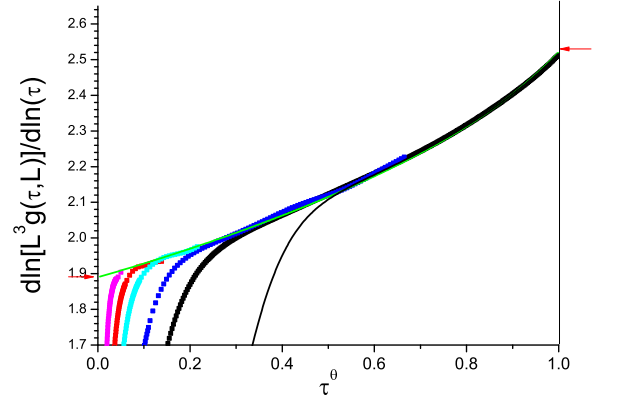


FIG. 12. (Color on line) BCC lattice. The temperature dependent effective normalized Binder cumulant exponent in the form $\partial \ln[L^3 g(\tau, L)]/\partial \ln \tau$ against τ . Data for $L = 48, 32, 24, 16, 12$ and HTSE from left to right. The HTSE curve is a 23 term sum of data from Ref. [18]. Green curve is the fit to the ThL data, calculated from Eq. (18).

with $\mu \sim 2.6$, see Figs. 15 and 16. The fit value for the critical amplitude can be compared to that estimated in Ref. [10], equivalent to $C_\xi = 1.077(12)$.

The ratios a_χ/a_ξ should be identical for these three models. The values estimated above are 1.22 for the FCC model, 1.32 for the BCC and 1.05 for the SC. The BCC model values for different spins S estimated in Ref. [10] were all close to 1.28. The present variations reflect the difficulties in extrapolating precisely so as to estimate the initial critical slopes.

For the normalized Binder parameter, as for the other

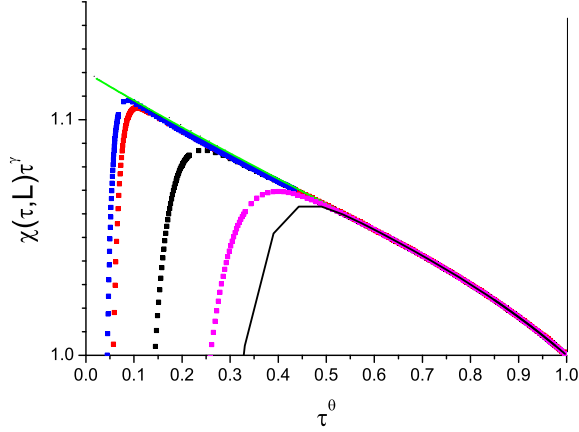


FIG. 13. (Color on line) SC lattice. Susceptibility data in the form $\chi(\tau, L)\tau^\gamma$ against τ^θ . Data for $L = 64, 48, 16, 8$ and HTSE from left to right. The HTSE curve is a 23 term sum of data from Ref. [18]. Green curve is the fit to the ThL data, see Eq. (19).

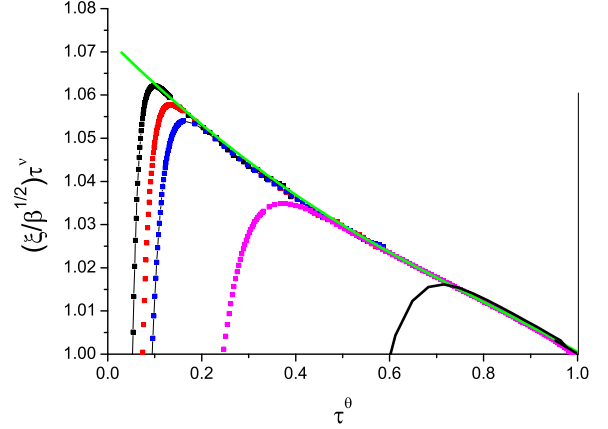


FIG. 15. (Color on line) SC lattice. Normalized correlation length data in the form $[\xi(\tau, L)/\beta^{1/2}]\tau^\nu$ against τ^θ . Data for $L = 48, 32, 16, 8$ from left to right. Green curve is the fit to the ThL data, see Eq. (20).

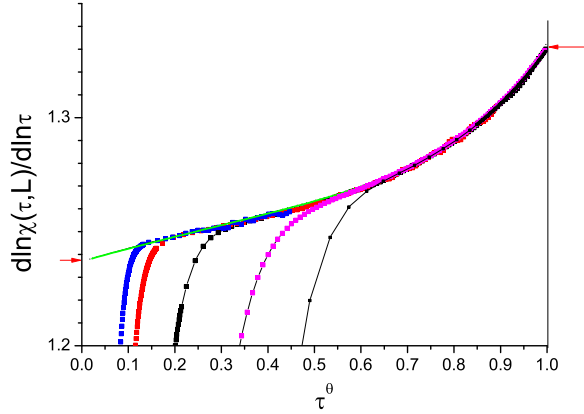


FIG. 14. (Color on line) SC lattice. The temperature dependent effective susceptibility exponent $\partial \ln \chi(\tau, L)/\partial \ln \tau$ against τ^θ . Data for $L = 48, 32, 16, 8$ and HTSE from left to right. The HTSE curve is a 23 term sum of data from Ref. [18]. Green curve is the fit to the ThL data, calculated from $\chi(\tau)$ in Eq. (19).

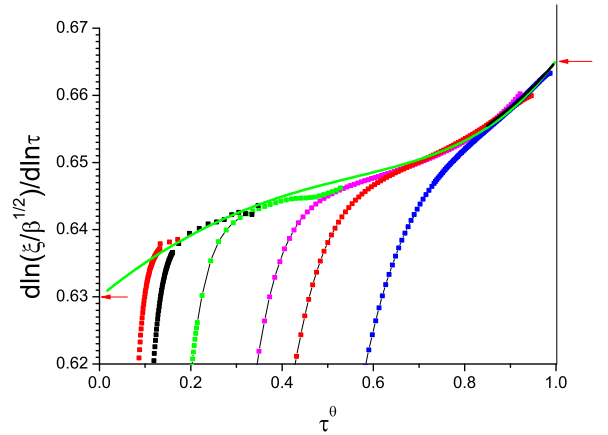


FIG. 16. (Color on line) SC lattice. The temperature dependent effective correlation length exponent $\partial \ln [\xi(\tau, L)/\beta^{1/2}]/\partial \ln \tau$ against τ^θ . Data for $L = 48, 32, 16, 12, 8, 6, 4$ from left to right. Green curve is the fit to the ThL data, calculated from Eq. (14).

lattices the standard leading correction term in τ^θ is missing. There is a strong analytic correction term linear in τ , accompanied by another strong term proportional to τ^μ with μ close to 2.85. All other terms are negligible so that

$$L^3 g(\tau, L) = 1.565\tau^{-3\nu} (1 - 0.27\tau - 0.096\tau^\mu) \quad (21)$$

with $\mu \sim 2.85$, see Figs. 17 and 18.

The SC normalized Binder cumulant data set provide the most favorable case from which to estimate the value

of the exponent μ , as the corresponding amplitude is strong, the leading confluent correction term is missing which simplifies the fit, and the HTSE data [18] are available for fitting the high-temperature region. We identify this μ with the subleading confluent correction exponent, so we estimate $\theta_2 = 2.85(5)$. All the fits to the data sets for this and the other models are compatible with a universal correction term being present having approximately this exponent. Obviously when the high exponent correction term amplitude is very weak, as the case for instance for the SC $\chi(\tau)$ and $\xi(\tau)/\beta^{1/2}$ data sets, the

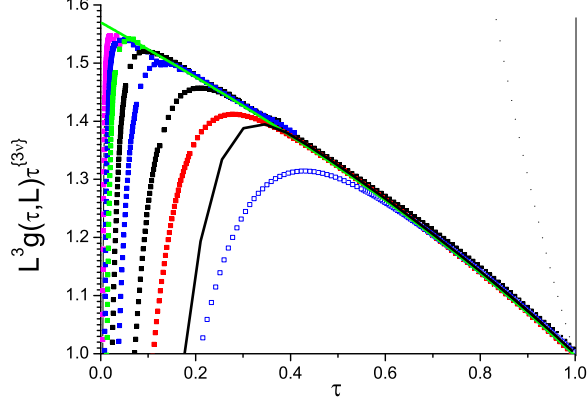


FIG. 17. (Color on line) SC lattice. Normalized Binder cumulant data in the form $L^3 g(\tau, L) \tau^{3\nu}$ against τ . Data for $L = 48, 32, 16, 12, 8, 6$, HTSE and 4 from left to right. The HTSE curve is a 23 term sum of data from Ref. [18]. Green curve is the fit to the ThL data, see Eq. (21).

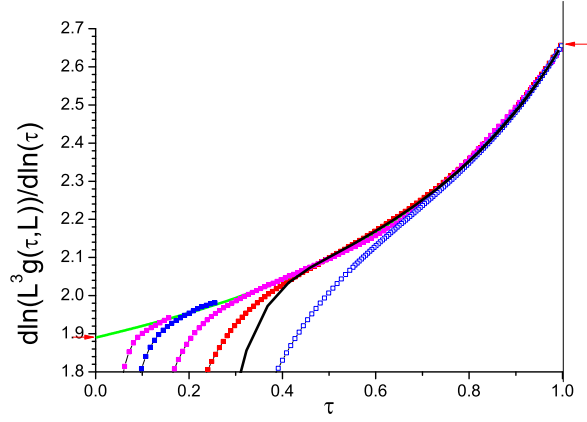


FIG. 18. (Color on line) SC lattice. The temperature dependent effective normalized Binder cumulant exponent in the form $\partial \ln[L^3 g(\tau, L)] / \partial \ln \tau$ against τ . Data for $L = 16, 12, 8, 6$, HTSE and 4 from left to right. The HTSE curve is a 23 term sum of data from Ref. [18]. Green curve is the fit to the ThL data, calculated from Eq. (21).

estimate for the corresponding μ is much more approximate. Nevertheless acceptable fits to these data sets also can only be made when a high-exponent correction term is included.

VI. DIAMOND LATTICE

In this lattice each site has 4 near neighbors and 8 sites per unit cell. The critical inverse temperature $\beta_c = 0.3697398(1)$ [21, 28]. For technical reasons it is

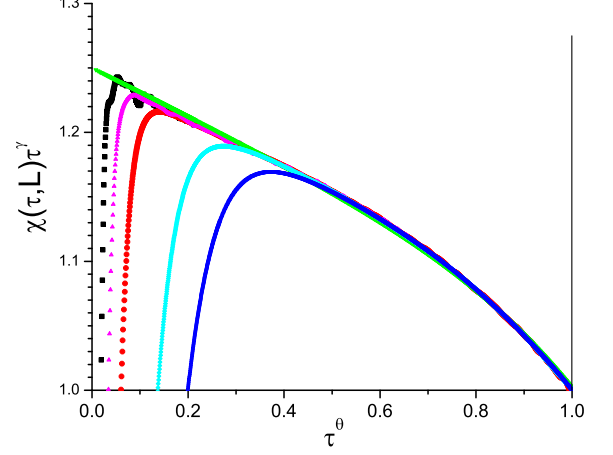


FIG. 19. (Color on line) Diamond lattice. Susceptibility data in the form $\chi(\tau, L) \tau^\gamma$ against τ^θ . Data for $L = 128, 64, 32, 12, 8$ from left to right. Green curve is the fit to the ThL data, see Eq. (22).

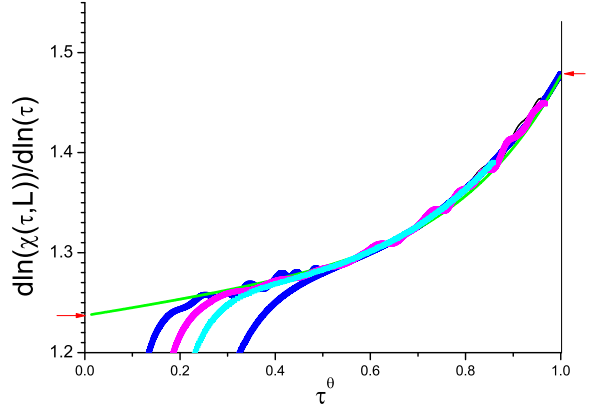


FIG. 20. (Color on line) Diamond lattice. The temperature dependent effective susceptibility exponent $\partial \ln \chi(\tau, L) / \partial \ln \tau$ against τ^θ . Data for $L = 24, 16, 12, 8$ from left to right. Green curve is the fit to the ThL data, calculated from $\chi(\tau)$ in Eq. (22).

more difficult to equilibrate and obtain accurate numerical data for this model. The ThL susceptibility $\chi(\tau)$ can be fitted satisfactorily with three correction terms :

$$\chi(\tau) = 1.250 \tau^{-\gamma} (1 - 0.147 \tau^\theta - 0.011 \tau - 0.04 \tau^\mu) \quad (22)$$

with $\mu \sim 2.8$, see Figs. 19 and 20. We do not dispose of sufficient data to analyse the normalized correlation length in this model.

The normalized Binder parameter behaves in much the same way as in the SC model. The leading correction term is strong and linear in τ , with a strong second term

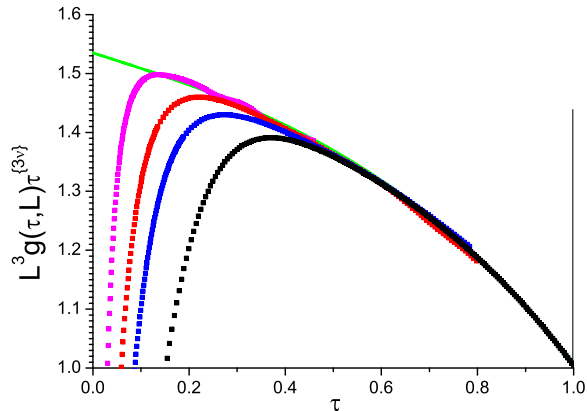


FIG. 21. (Color on line) Diamond lattice. Normalized Binder cumulant data in the form $L^3 g(\tau, L) \tau^{3\nu}$ against τ . Data for $L = 12, 8, 6, 4$ from left to right. Green curve is the fit to the ThL data, see Eq. (23).

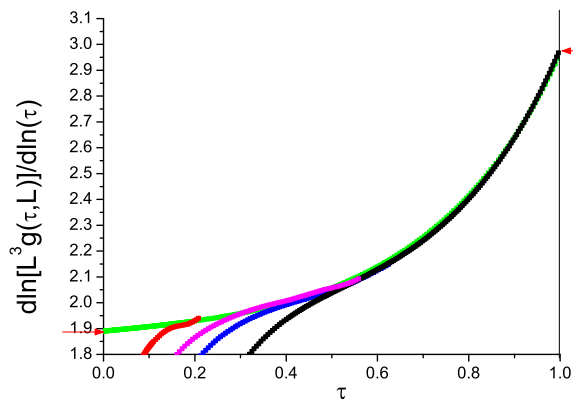


FIG. 22. (Color on line) Diamond lattice. The temperature dependent effective normalized Binder cumulant exponent in the form $\partial \ln[L^3 g(\tau, L)] / \partial \ln \tau$ against τ . Data for $L = 12, 8, 6, 4$ from left to right. Green curve is the fit to the ThL data, calculated from Eq. (23).

proportional to τ^μ with $\mu \sim 2.9$ to a good approximation so

$$L^3 g(\tau, L) = 1.535 \tau^{-3\nu} (1 - 0.157\tau - 0.186\tau^\mu), \quad (23)$$

see Figs. 21 and 22. The μ correction term amplitude is even stronger than for the SC model, and although no HTSE data are available for this model the estimate for μ is fully consistent with the SC and BCC model Binder cumulant analyses.

VII. CONCLUSION

We measure the susceptibility, normalized second-moment correlation length, and normalized Binder-cumulant data for the 3D spin-1/2 FCC, BCC, SC and diamond Ising models, covering the entire paramagnetic temperature range. We treat the bootstrap values for the principle critical exponents as exact and carry out three term (or two term for the normalized Binder cumulant) fits adjusting the critical amplitudes, the correction-term amplitudes, and a high-order term exponent μ . The critical amplitudes and correction-term amplitudes evolve regularly from one model to the next as functions of the numbers of nearest neighbors, with the susceptibility and correlation-length critical amplitudes becoming systematically stronger as the number of neighbors drops. Amplitude ratios for the leading confluent correction terms for different observables such as a_χ/a_ξ are universal. Our estimates for this ratio are broadly compatible with a value ~ 1.25 [10] (though the value of this particular ratio turns out to be hard to estimate accurately).

This universality implies that if for an observable $Q(\tau)$, $a_q = 0$ for one particular model then a_q must also be equal zero for all other models in the same universality class. The data show that this rule is indeed obeyed for the normalized Binder parameter in all four models studied; the leading confluent correction term $a_g \tau^\theta$ is absent to within the statistical uncertainty. As the normalized Binder parameter is equal to $-\chi_4(\tau)/(2\chi(\tau)^2)$ the correction Binder-cumulant amplitude ratio being equal to zero is equivalent to $a_{\chi_4}/a_\chi = 2$ for the 3D Ising universality class. The normalized Binder cumulant analytic corrections $b\tau$ are always strong but decrease progressively as the number of neighbors drops. The further normalized Binder cumulant $c\tau^\mu$ correction term passes progressively from negligible for the FCC lattice to very strong for the SC and Diamond lattices, with $\mu = 2.85(10)$ consistently.

Because of the absence of the standard $a\tau^\theta$ term for the normalized Binder parameter and the strength of the $c\tau^\mu$ term in all cases except FCC these estimates of μ are the most reliable among the various data sets. All other high-order "minor" term amplitudes appear to be negligible in all cases.

The estimates of μ from the susceptibility and correlation length data are less accurate than the Binder cumulant values because of the more delicate play-offs in the analyses between the three correction term amplitudes and the value of μ , but in each case to within the uncertainty the μ estimates are consistent with the optimal Binder cumulant value. We identify this optimal overall $\mu = 2.85(5)$ with the subleading thermal confluent correction exponent τ_2 . Hence we estimate the second confluent correction exponent $\omega_2 = \theta_2/\nu \sim 4.50(10)$ and the bootstrap $\Delta_{\epsilon''} = 3 + \omega_2 \sim 7.50(10)$. These values are consistent with the range of published bootstrap theory estimates : $\omega_2 \sim 4$ [2], $\Delta_{\epsilon''} = 7.27(5)$ [3], $\Delta_{\epsilon''} = 7.60$ [4].

A recent bootstrap calculation, Ref. [29] Table 2, provides a high precision estimate for the ϵ'' stable operator

parameter $\Delta = 6.8956(43)$ which can be translated to give the second thermal conformal correction exponent $\theta'' = 2.454(3)$. The value that we have estimated numerically is $2.85(5)$ so rather higher. In the analysis of the numerical data we assumed from the outset that yet higher order correction terms were of negligible amplitude. The small inconsistency between the bootstrap and numerical values for θ'' can be understood if in fact one or more of the neglected still higher order term or terms are of weak but not quite negligible amplitude.

ACKNOWLEDGMENTS

We would like to thank D. Simmons-Duffin, P. Butera, S. Rychkov and Y. Nakayama for helpful comments. The computations were performed on resources provided by the Swedish National Infrastructure for Computing (SNIC) at the High Performance Computing Center North (HPC2N) and Chalmers Centre for Computational Science and Engineering (C3SE).

-
- [1] S. El-Showk, M. F. Paulos, D. Poland, S. Rychkov, D. Simmons-Duffin and A. Vichi, *Phys. Rev. D* **86**, 025022 (2012).
 - [2] S. El-Showk, M. F. Paulos, D. Poland, S. Rychkov, D. Simmons-Duffin and A. Vichi, *J. Stat. Phys.* **157**, 869 (2014).
 - [3] F. Gliozzi, P. Liendo, M. Meineri, A. Rago, *JHEP* **05**, 036 (2015).
 - [4] Y. Nakayama, *Phys. Rev. Lett.* **116**, 141602 (2016).
 - [5] F. Kos, D. Poland and D. Simmons-Duffin, *JHEP* **11**, 109 (2014).
 - [6] D. Simmons-Duffin, *JHEP* **06**, 174 (2015).
 - [7] K. E. Newman and E. K. Riedel, *Phys. Rev. B* **30**, 6615 (1984).
 - [8] C. Domb and M.F. Sykes, *Phys. Rev.* **128**, 168 (1962).
 - [9] F. Wegner, *Phys. Rev. B* **5**, 4529 (1972).
 - [10] P. Butera and M. Comi, *Phys. Rev. B*, **65**, 144431 (2002).
 - [11] M. Hasenbusch *Phys. Rev. B* **82**, 174433 (2010).
 - [12] M. Ferer, *Phys. Rev. B* **16**, 419 (1977).
 - [13] M.C. Chang and A. Houghton, *Phys. Rev. B* **21**, 1881 (1980).
 - [14] M. Campostrini, M. Hasenbusch, A. Pelissetto, and E. Vicari, *Phys. Rev. B* **74**, 144506 (2006).
 - [15] J. -K. Kim, A. J. F. de Souza and D. P. Landau, *Phys. Rev. E* **54** 2291 (1996).
 - [16] V. Privman and M. E. Fisher, *Phys. Rev. B* **30**, 322 (1984).
 - [17] I. A. Campbell, K. Hukushima, and H. Takayama, *Phys. Rev. Lett.* **97**, 117202 (2006).
 - [18] P. Butera and M. Comi, arXiv:0204007 (2002) (unpublished).
 - [19] V. Privman, P. C. Hohenberg and A. Aharony, *Universal Critical-Point Amplitude Relations, in Phase Transitions and Critical Phenomena* (Academic, NY, 1991), eds. C. Domb and J. L. Lebowitz, **14**, 1.
 - [20] R. Häggkvist, A. Rosengren, P. H. Lundow, K. Markström, D. Andrén, and P. Kundrotas, *Adv. Phys.* **56** 653 (2007).
 - [21] P. H. Lundow, K. Markström, and A. Rosengren, *Phil. Mag.* **89**, 22 (2009).
 - [22] P. H. Lundow and I. A. Campbell, *Phys. Rev B* **83**, 184408 (2011).
 - [23] E. Luijten, H. W. J. Blöte, and K. Binder, *Phys. Rev. Lett.* **79**, 561 (1997).
 - [24] E. Luijten, *Phys. Rev. E* **59**, 4997 (1999).
 - [25] P. H. Lundow and I. A. Campbell, *Phys. Rev B* **83**, 014411 (2011).
 - [26] Y. Murase and N. Ito, *J. Phys. Soc. Jpn.* **77**, 014002 (2008).
 - [27] H. W. J. Blöte, E. Luijten and J. R. Heringa, *J. Phys. A: Math. Gen.* **28**, 6289 (1995).
 - [28] Y. Deng and H. W. J. Blöte, *Phys. Rev. E* **68** 036125 (2003).
 - [29] D. Simmons-Duffin, *JHEP* **03**, 86 (2017).